Journal of Archaeological Science 53 (2015) 190–201

Contents lists available at ScienceDirect

Journal of Archaeological Science

journal homepage: http://www.elsevier.com/locate/jas

Consolidation or initial design? Radiocarbon dating of ancient iron alloys sheds light on the reinforcements of French Gothic Cathedrals

Stéphanie Leroy [a, *], Maxime L'Héritier [b], Emmanuelle Delqué-Kolic [c], Jean-Pascal Dumoulin [c], Christophe Moreau [c], Philippe Dillmann [a]

[a] Laboratoire Archéomatériaux et Prévision de l'Altération (LAPA), IRAMAT LMC UMR 5060 CNRS, and SIS2M UMR 3299 CEA/CNRS, CEA Saclay, 91191 Gif-sur-Yvette Cedex, France
[b] Université de Paris 8, Département d'histoire, EA 1571: Histoire des Pouvoirs Savoirs et Sociétés, 93526 Saint-Denis, France
[c] Laboratoire de Mesure du Carbone 14 (LMC14), UMS 2572 CNRS, CEA Saclay, 91191 Gif-sur-Yvette Cedex, France

ARTICLE INFO

Article history:
Received 19 June 2014
Received in revised form
6 October 2014
Accepted 18 October 2014
Available online 27 October 2014

Keywords:
Radiocarbon dating
Iron reinforcements
Gothic Cathedrals

ABSTRACT

Large quantities of iron reinforcements, found in most Gothic monuments, are a data source for the interpretation of medieval architecture however their role both in contemporary engineering theory and the technical reality of construction yards has not yet been specified due to the difficulty of directly dating them. We present here an original radiocarbon dating methodology to date metal itself. Radiocarbon dates were measured for iron reinforcements used in specific parts of Bourges and Beauvais cathedrals, two iconic buildings in the development of French gothic architecture. Coupled with archaeometric and archaeological data, the new chronological results illuminate the major and active roles played by iron in the strategy of the building yards. At Bourges, iron was assimilated into the cathedral's construction strategy, whereas at Beauvais iron was integrated from the initial design, added to the monument following the vicissitudes of the building yard, and still used during the modern period. Thus, through decisive advances in radiocarbon dating of iron artefacts, the evolution of medieval architectural and engineering thought and action has been more reliably reconstructed.

1. Introduction

It is now currently understood that most gothic cathedrals and churches can no longer be considered as structures of purely lithic design. In addition to stone, the use of large quantities of iron or steel reinforcements, clamps as well as chains and tie-rods of substantial size has been brought to light by recent historical and archaeological researches (Chapelot and Benoit, 1985; Bernardi and Dillmann, 2005; L'Héritier et al., 2010, L'Héritier, 2007; Timbert, 2009). Thus, at Soissons, Paris, Rouen, Beauvais, and Bourges metal was potentially considered being part of the initial constructive design considering archaeological evidence from construction analysis (Erlande-Brandenburg, 1996; Taupin, 1996; Férauge and Mignerey, 1996) and archaeometry that brought light the use of ancient processes to produce metal components (Dillmann and L'Héritier, 2007; Dillmann, 2009; L'Héritier et al., 2010). Unfortunately, the history of medieval monuments beginning with their construction is often tumultuous, given the succession of building phases since the medieval period for the purposes of modification, repair and conservation. Each of these medieval, modern or contemporary building yards potentially used metal, thereby often making the archaeological interpretations of a building limited in this respect. At this stage, the absolute dating of these iron elements is essential for specifying their place both in medieval constructive thought and the technical reality of construction building yards. The aim of the present paper is to propose an original methodology for radiocarbon dating to examine reinforcing elements discovered in Bourges and Beauvais Cathedrals, two major monuments in the development of French gothic architecture in which ferrous alloy armatures of significant size (*i.e.* tie-rods and chains) have been identified.

The basic idea for dating ferrous alloys by radiocarbon is that the carbon contained in the steely zones of the ancient metal, coming from the charcoal used during ore smelting, can be extracted and its isotopic ratio determined, leading to a radiocarbon date. With the advent of accelerator mass spectrometry (AMS), dating of archaeological samples of a few milligrams has become technically feasible (Cook et al., 2003a). With uncertainties (see below), the

* Corresponding author. Tel.: +33 1 69 08 90 67.
E-mail address: stephanie.leroy@cea.fr (S. Leroy).

http://dx.doi.org/10.1016/j.jas.2014.10.016
0305-4403/

radiocarbon dates correspond to the manufacturing date of the artefact. Nevertheless, only a hundred iron samples have been dated by radiocarbon and published to date (Van der Merwe and Stuiver, 1968; Cresswell, 1992; Kusimba et al., 1994; Beukens et al., 1999; Cheoun et al., 2001; Cook et al., 2001; Craddock et al., 2002; Hüls et al., 2004; Oinonen et al., 2009) and ~15% of the dates obtained seemed to be unreliable (Cook et al., 2003a). This discrepancy could be due to different factors: the age of the wood used to produce the charcoal (Forbes, 1955, 1963, 1964; Kusimba et al., 1994), potential contamination with the carbonates of the ore, recycling of older metals, cementing with other materials containing carbon. Another major limitation is related to the low carbon content of bloomery iron obtained in the Middle Ages, heterogeneously distributed within the metallic matrix. This stresses the necessity of having a good knowledge of the nature of the material prior to attempt dating. Another difficulty is linked to the carbon extraction from the sample. The protocols explored since the 1960's (Cook et al., 2003a) are based on a preliminary chemical cleaning or mechanical preparation to abrade, cut or mill the artefact (Cook et al., 2003b; Hüls et al., 2004; Oinonen et al., 2009). Various approaches for extracting carbon were then used based on acidic dissolution of iron (Nakamura et al., 1995; Scharf et al., 2004), and combustion without (Van der Merwe and Stuiver, 1968; Cresswell, 1992) or with acidic pre-cleaning (Cook et al., 2001; Scharf et al., 2005). Scharf et al. (2005) also proposed making a metal/carbon mix ready to be directly measured by AMS. This method is unfortunately not adapted to samples with relatively low C content such as ancient bloomery iron. None of these approaches consider the microscopic heterogeneity of bloomery iron and the fact that important zones of the artefact could contain very low C content, considerably lowering the chances of randomly sampling significant quantities of iron. Considering these different risks of misdating, we set up an adapted methodology for dating bloomery iron found in cathedrals following a detailed metallographic and Slag Inclusions (SI) study performed in transverse sections of the artefacts (Pagès et al., 2011). This approach allows for the determination of the chemical composition of SI entrapped in the metal providing information on the iron-making process and potential cementing and recycling of the archaeological object (Dillmann and L'Héritier, 2007; Fluzin et al., 2011). This methodology was validated on artefacts of known age from different periods and obtained with different kinds of ores including carbonated ones. We then examined the resulting ^{14}C data for iron reinforcements in Bourges and Beauvais Cathedrals, with regard to their location in the structure of the cathedrals.

2. Methods

2.1. Experimental procedure

All objects were cross-sectioned and polished to expose both the metallic matrix and the SI entrapped in the metal. By working on cross-sections, we excluded any pollution due to rust that could be a source of carbon contamination (Cresswell, 1992; Scharf et al., 2005). The procedure consists of first performing a metallographic observation of the matrix of the polished cross-section under an OLYMPUS light microscope (BX51 model) under reflected light to visualise the possible welding lines. This step was followed by analysis of SI entrapped in the metal to get information on the manufacture of the object, especially identifying use of metal pieces of different provenances (recycling) (Dillmann and L'Héritier, 2007). The chemical analysis of the SI is performed by X-rays Energy Dispersive Spectrometry coupled to a Scanning Electron Microscope. The SI analytical methodology will not be detailed here and can be found in Pagès et al. (2011), Leroy et al. (2012), Disser et al. (2014). A second metallographic etching was then done on the polished cross-section using Nital 4% to reveal the distribution of the carbon content within the metal allowing us to sample in the highest carburized zones for ^{14}C dating. It was also verified that no evidence of cementation could be observed. The chemical cleaning by nitric acid (HNO_3) also permitted removal of the outer surface and enhanced the elimination of possible carbon pollution that could have been added during cutting or polishing. Each cross-section was finally washed with de-ionized water, followed by ethanol washes and then dried to suppress any carbon contamination in an oven at 80 °C. The conditions required for each step of this preparation are described in Table 1.

Table 1
Sample treatment conditions used on the iron artefacts during the sampling procedure.

Step	Treatment	Remark
Cutting	SiC saw blade	Cross-section Exclusion of corrosion layer sampling
Polishing_1	SiC abrasive papers	
Polishing_2	Diamond paste	
Metallographic observation_1	4% HNO_3 etching	Revelation of metallic matrix microstructure + welding line location
Polishing_3	Diamond paste	
SI analyses		Information about manufacture of the object + identification of recycling case
Polishing_4	Diamond paste	
Cleaning_1	EtOH x2 + US 10 min	
Metallographic observation_2 (Cleaning_2)	4% HNO_3 etching	Revelation of the carbon distribution
Cleaning_3	H_2O	
Cleaning_4	EtOH	
Drying	80 °C	
Cleaning_5	Surface short abrasion + drill	In the highest carburized zones
Sampling	Ceramic/TiN or CoB coated drills	In the highest carburized zones

After this preparation, we collected samples in the highest carburized zones with ceramic, TiN or CoB coated drills of several millimetre diameters (Ø2 mm, Ø2.5 mm, Ø3.5 mm). Particles collected are under powder or shavings less than 1 mm thick. To ensure the elimination of potential carbon contamination, a first short abrasion with the drill was done to remove the outer layer of iron prior to the final sampling. The extracted particles were then picked up with a magnet. We finally sampled the weight required (a few hundred milligrams) to obtain up to 1 mg of carbon when

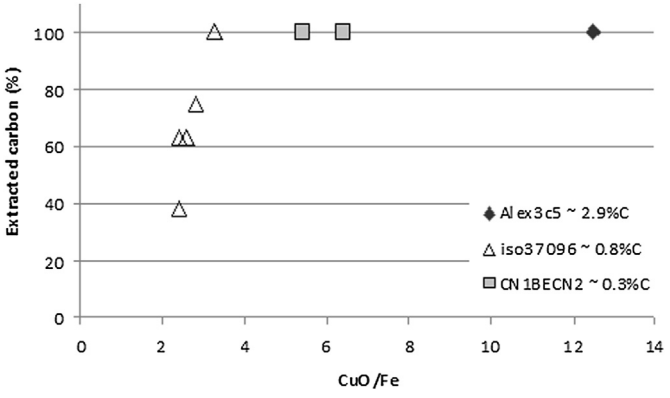

Fig. 1. Carbon extraction efficiency (%) as a function of CuO/Fe ratio values for samples with various carbon contents ($T = 850$ °C for 5 h).

Table 2
Radiocarbon dates of «blank» test samples and average value for the ^{14}C free charcoal.

Sample	Sub-sample	Lab.ID SacA	% C	$\delta^{13}C$ (‰)	pMC	Radiocarbon age (BP)
Cast iron from Alexandre III bridge (Paris)	Alex3c5_1	16739	2.9/3	−27.4	3.49 ± 0.05	29,960 ± 13
	Alex3c5_2	16740		−27.5	3.02 ± 0.05	28,120 ± 12
	Alex3c5_3	16742		−21.2	2.96 ± 0.05	28,265 ± 13
	Alex3c5_4	16743		−20.0	2.89 ± 0.05	28,465 ± 14
Contemporary cast iron	FI_1	18746	3.2	−22.9	3.73 ± 0.04	26,427 ± 95
	FI_2	18747		−27.7	3.24 ± 0.07	27,565 ± 17
	FI_3	19723		−24.7	2.77 ± 0.05	28,810 ± 15
^{14}C free charcoal		18745	–	−16.4	0.38 ± 0.01	44,785 ± 29
^{14}C free charcoal		Average value	–	–	0.33 ± 0.12	46,555 ± 32

possible, which means 125 mg for eutectoid (0.8% of C) steel and 1 g for low carbon iron (0.1% of C). When feasible, a small amount of the sample (~3 mg) was analysed in an EA (Elemental Analyzer) to determine the carbon content of the sample. This value was used to estimate the combustion yield by comparing the %CT (Carbon Total) value of the sample and the amount of CO_2 produced.

A sufficient quantity of the sample (up to 300 mg) was sealed in a clean quartz tube (original diameter: 20 × 0.5 cm; diameter after welding: 12 × 0.5 cm) along with an excess of CuO as an oxidizing agent and a 1 cm silver wire to trap undesired elements such as chlorine and sulphur which can poison the graphitisation. We tested various CuO/Fe ratios to ensure complete oxidation of the iron. Fig. 1 reports the results of the combustion yields obtained for steel (0.2–0.8% of C) and cast iron (3% of C) samples with various excesses of oxygen ($2.4 < CuO/Fe < 12.5$). When $CuO/Fe > 3$, over 90% of the initial carbon was extracted as shown by CN1BECN2 and Alex3c5-4 results. As recommended by Hüls et al. (2004), we performed combustion with a CuO/Fe ratio of 5 to provide a sufficient excess of oxygen in the tube during combustion and ensure the extraction of the original carbon.

The quartz tube was then sealed and burned at 850 °C for 5 h and cooled slowly during the night. Finally, sealed tubes were cracked on an automatic line and the CO_2 gas produced was cryogenically (liquid nitrogen) stored in vials. When the sample was larger than 300 mg, it was fractionated into several tubes to keep enough volume empty for the gas production and to avoid blowing the tube during combustion. The CO_2 fractions which evolved from each tube were then gathered in a single vial to reach between 0.5 and 1 mg of CO_2. The CO_2 samples were finally automatically graphitized at the LMC14 laboratory according to the protocol described by Cottereau et al. (2007). The ^{14}C measurements were performed with ARTEMIS, the AMS facility installed in Saclay

Fig. 2. Sample iso37096 from Castel-Minier archaeological site (Ariège, France). Schematic drawing of the microscopic metallographic observation on the cross-section after Nital etching.

Table 3
Radiocarbon dates of charcoal fragments used for the experimental reduction (internal ring, external ring, taken in the experimental bloom).

Sample	Lab.ID	$\delta^{13}C$ (‰)	pMC	Calibrated age (2σ, 95.4%)
Charcoal 1 internal ring	SacA.26324	−31.8	106.42 ± 0.35	Post 2003
Charcoal 1 external ring	SacA.26325	−32.4	105.69 ± 0.36	Post 2004
Charcoal 2 internal ring	SacA.26326	−30.9	106.31 ± 0.36	Post 2003
Charcoal 2 external ring	SacA.26327	−30.7	105.32 ± 0.36	Post 2005
Charcoal 3	Ly-15712	−27.05	106.94 ± 0.71	Modern
Charcoal 1 from bloom	SacA.28384	−17.3	108.13 ± 0.59	Post 1999
Charcoal 2 from bloom	SacA.28385	−27.6	106.49 ± 0.41	Post 2002

(France) (Cottereau et al., 2007). The ^{14}C contents are expressed in pMC and the radiocarbon age given in BP (Stuiver and Polach, 1977). Data were corrected for isotopic fractionation measured in the AMS. Calendar age ranges were calculated using Oxcal 4.2 (Bronk Ramsey, 2009; Bronk Ramsey and Lee, 2013) in conjunction with the data set IntCal 09 (Reimer et al., 2009).

For all samples, a background value corresponding to the level of ^{14}C contamination occurring during the preparation steps is subtracted from the AMS result. These background values are regularly measured thanks to blank samples, *i.e.* ^{14}C-free materials of a similar nature as the unknown samples measured. We first tested cast irons elaborated with coal and thus, normally free of ^{14}C: a cast iron sample from the decoration of the Alexandre III bridge in Paris built in 1900 and a contemporary cast iron. Several aliquots of a ^{14}C-free charcoal (a charcoal from a site of South Africa (Border Cave)) used as blank sample at LMC14 (Hatté et al., 2003; Cottereau et al., 2007) were also combusted in the same conditions. Surprisingly, results presented in Table 2 show that the ^{14}C content is much higher for cast irons than for the ^{14}C free charcoal. These "high" radiocarbon contents have already been observed by Cresswell (1992), Nakamura et al. (1995) and Hüls et al. (2004) and seem to be induced by the manufacturing of these samples. We therefore decided to use the average value of the ^{14}C contents measured for ^{14}C free charcoals (grey line in Table 2) as the background value.

2.2. Validation of the procedure with objects of known age

A specific set of well-dated artefacts was selected to test our experimental procedure. The first one is a medieval nail (iso37096) from the Castel-Minier site (Ariège, France) from the 16th century with a *Terminus Ante Quem* (TAQ) of 1580 AD according to the archaeological excavations (Téreygeol, 2011; Leroy et al., 2012). Despite the nail is mainly constituted of ferrite, metallographic analyses allowed us to locate zones with $\%C > 0.3$ where the ^{14}C sampling could be performed (Fig. 2). The second artefact is a Gallo-Roman iron ingot (SM2 1/1) from the shipwreck of Les-Saintes-Maries-de-la-Mer (France) dated from late 1st c. BC to 1st c. AD by amphorae (Pagès et al., 2011). These bars were submitted to extensive metallographic investigations (see Pagès et al., 2011) allowing us to locate the carburised zones ($\%C > 0.3$) on transverse sections.

Two other samples were chosen to specifically test the possibility of pollution by geological carbon from carbonate siderite ores ($FeCO_3$) sometimes used in ancient iron making (Cresswell, 1992; Craddock et al., 2002; Oinonen et al., 2009). Some authors claims that a part of carbon from this geological carbonates could enter the iron and consequently significantly hinder the age measurement (Craddock et al., 2002). Actually, the thermal dissociation temperature of siderite is 520 °C (Bugayev et al., 2001) and is very low compared to that of the shaft furnaces (<1300 °C). Geological carbon would be eliminated under the form of CO_2 at the top of the

Table 4
Radiocarbon dates of archaeological known age samples and of the experimental bloom.

Sample	Sub-sample	Lab.ID SacA	Drill	% C	Extracted carbon content (mg)	pMC	Radiocarbon age (BP)	Calibrated age (2σ, 95.4%)	Archaeological age
SM2.1/1	SM2.1.1-0	19725	Ceramic	0.7–0.8	1.20	78.34 ± 0.24	1961 ± 25	39 BC – 115 AD	Late 1st c. BC – 1st c.AD
	SM2.1.1-a	26489	Ceramic		1.15	77.46 ± 0.22	2051 ± 23	163 BC – 5 AD	
	SM2.1.1-b	26490	Ceramic		0.79	77.99 ± 0.24	1997 ± 24	46 BC – 61 AD	
	SM2.1.1-c	26491	TiN coated		1.40	77.90 ± 0.21	2006 ± 21	48 BC – 53 AD	
	SM2.1.1-d	26492	TiN coated		1.03	77.55 ± 0.23	2042 ± 24	158 BC – 22 AD	
	SM2.1.1-f	26494	TiN coated		1.27	78.03 ± 0.24	1993 ± 24	45 BC – 62 AD	
	SM2.1.1-g	26495	TiN coated		1.28	77.90 ± 0.24	2006 ± 25	53 BC – 61 AD	
	SM2.1.1-h	26496	BoC coated		0.89	78.26 ± 0.22	1969 ± 23	39 BC – 77 AD	
	SM2.1.1-i	26497	BoC coated		1.07	78.00 ± 0.23	1995 ± 24	46 BC – 62 AD	
	SM2.1.1-j	26498	BoC coated		1.42	77.95 ± 0.26	2001 ± 27	51 BC – 65 AD	
	SM2.1.1-k	26499	TiN coated		1.46	77.86 ± 0.27	2011 ± 28	91 BC – 64 AD	
	SM2.1.1-l	26500	TiN coated		1.27	78.03 ± 0.24	2080 ± 27	182 – 4 BC	
iso37096	iso37096-i 1	23176	TiN coated	0.8	0.56	95.25 ± 0.24	391 ± 20[a]	1445 – 1512 AD	1500–1580 AD
	iso37096-i 3	23178	TiN coated		1.00	95.66 ± 0.31	356 ± 25[a]	1453 – 1582 AD	
	iso37096-i 4	23179	TiN coated		0.98	95.36 ± 0.23	381 ± 20[a]	1447 – 1518 AD	
	iso37096-i 5	23180	TiN coated		0.84	95.56 ± 0.22	365 ± 20[a]	1452 – 1581 AD	
	iso37096-i 7	23182	TiN coated		1.32	95.63 ± 0.31	359 ± 25[a]	1451 – 1583 AD	
	iso37096-i 10	23185	Ceramic	<0.05	0.24	95.56 ± 0.26	365 ± 20[a]	1451 – 1582 AD	
GL03-24	GL03-24-1	26699	TiN coated	>2%	0.85	95.22 ± 0.34	394 ± 29	1446 – 1615 AD	1480–1580 AD
	GL03-24-2	26700	TiN coated	>2%	0.48	95.54 ± 0.34	367 ± 28	1456 – 1620 AD	
	GL03-24-3	26701	TiN coated	>2%	0.67	96.35 ± 0.35	298 ± 29	1522 – 1647 AD	
	GL03-24-4	26702	TiN coated	>2%	0.76	96.05 ± 0.34	324 ± 28	1516 – 1636 AD	
	GL03-24-5	26703	TiN coated	>2%	0.54	96.05 ± 0.41	324 ± 34	1515 – 1638 AD	
RED2	RED2-2	28465	TiN coated	0.3–0.5	0.36	106.13 ± 0.30		Post 2003	Post 2000
	RED2-4	28979	TiN coated		0.23	105.43 ± 0.44		Post 2004	

[a] For the medieval nail iso37096, the calibrated ages were constrained to be earlier than 1580 ± 5 AD as a Terminus Ante Quem (TAQ) as indicated by archaeological findings.

furnace and would therefore not be involved in the reduction process taking place at the bottom of the furnace. To verify this hypothesis, we dated a cast iron sample (GL03-24) from the medieval reduction site of Glinet, in activities between 1480 and 1580 AD (Arribet-Deroin, 2001), and obtained from sideritic ore as demonstrated in Desaulty (2008). In addition, we experimentally obtained iron using unroasted siderite and charcoal made especially for the smelting. The proportion of ^{14}C varied a lot over the last 50 years but has stabilised over the last 10 years. For the experimental reduction, we therefore used young wood (under 10 years) for the charcoal to be able to detect and quantify with precision any possible geological carbon pollution on the dating results. To ensure that no contamination was added during the charcoal production steps, we dated different fragments taken from the internal and external rings of the wood. Fragments of charcoal found in the obtained experimental bloom were also dated (Table 3). A measurement was performed at the Radiocarbon Dating Laboratory in Lyon (France). ^{14}C activities were calibrated

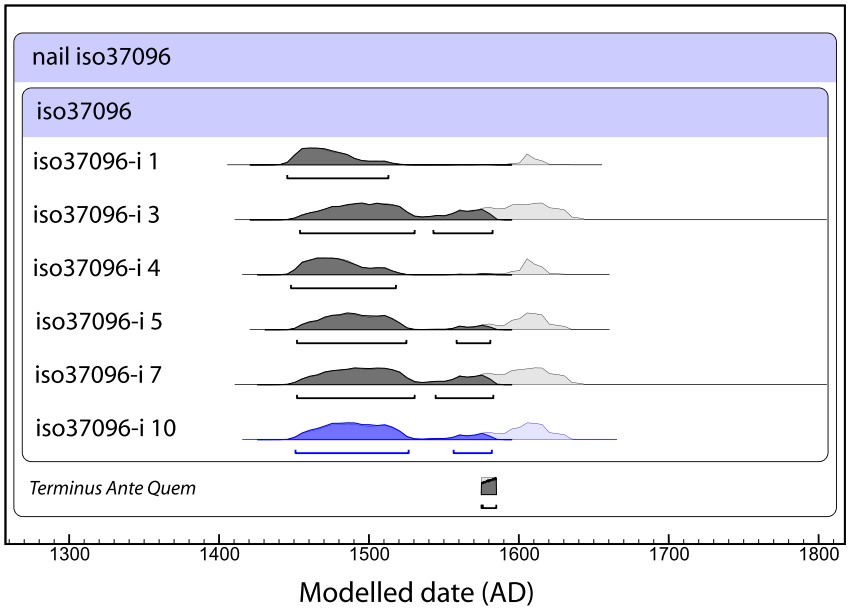

Fig. 3. Calibrated ages for the sub-samples of iso37096. Ages are represented by the probability densities whose shape depends on the calibration curve. The hollow distributions show the unmodeled calibrated probabilities and the solid distributions show the reduced probability distributions after applying the TAQ constraint. In grey: samples collected with a TiN coated drill. In blue: sample collected with a ceramic drill. Calendar age ranges were calculated using Oxcal 4.2 (Bronk Ramsey, 2009; Bronk Ramsey and Lee, 2013) and the IntCal09 calibration curve (Reimer et al., 2009). (For interpretation of the references to colour in this figure legend, the reader is referred to the web version of this article.)

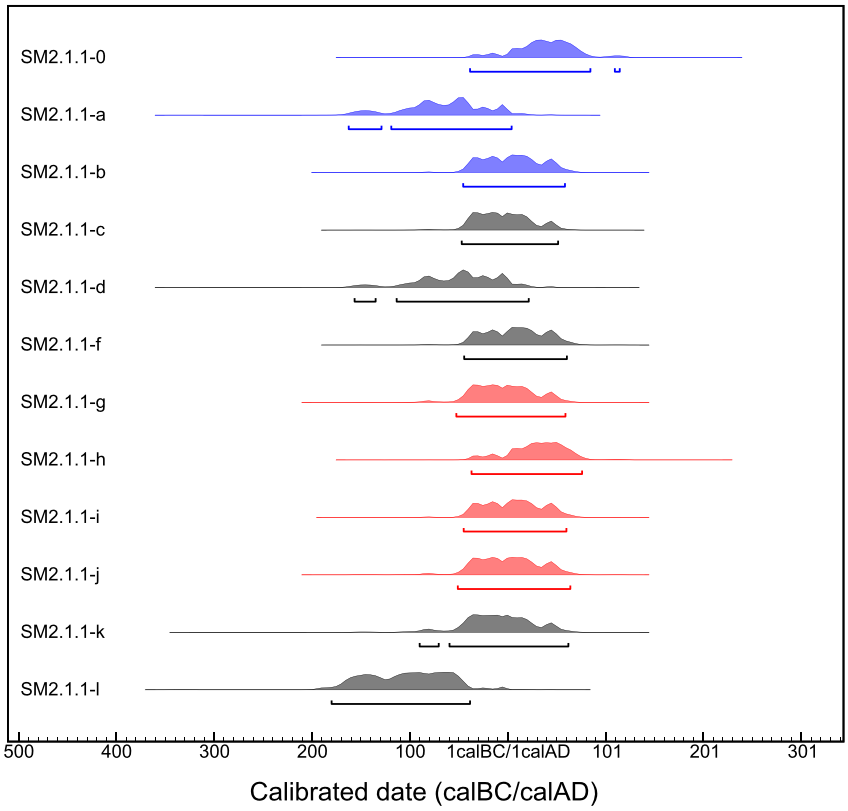

Fig. 4. Calibrated ages for the sub-samples of SM2.1/1. Ages are represented by the probability densities whose shape depends on the calibration curve. In blue: samples collected with a ceramic drill. In grey: samples collected with a TiN coated drill. In red: samples collected with a CoB drill. Calendar age ranges were calculated using Oxcal 4.2 (Bronk Ramsey, 2009; Bronk Ramsey and Lee, 2013) and the IntCal09 calibration curve (Reimer et al., 2009). (For interpretation of the references to colour in this figure legend, the reader is referred to the web version of this article.)

with the online program CaliBomb using the calibration curve of Levin and Kromer established for the mid-latitudes of the northern hemisphere. The results clearly show that the dates obtained are modern. This charcoal is therefore a good chronological marker for detecting possible contamination of the geological carbon in the final experimental product. The obtained experimental bloom (RED2) was studied on cross-section to locate and sample (RED2.2 and RED2.4) in the most carburised zones following the procedure detailed above.

The resulting radiocarbon dates of the resulting graphite for samples of known age are showed in Table 4, Figs. 3 and 4. By using the R_Combine function in OxCal 4.2 (Bronk Ramsey and Lee, 2013; Bronk Ramsey, 2009), radiocarbon ages measured on the different sub-samples from iso37096 and SM2.1/1 are shown to be statistically consistent, passing a χ^2-test at 95% confidence. The combined dates are respectively 1456–1513 calAD for nail iso37096 and 45 calBC-19 calAD for ingot SM2.1/1. The direct radiocarbon dates of the iron fit perfectly into the archaeological chronological contexts. This regularity in ^{14}C dates and their consistency with the archaeological records therefore confirm that no significant contamination of exogenous carbon was introduced with our protocol.

Concerning samples dedicated to the study of the influence of carbonated ores, the resulting radiocarbon dates of cast iron GL03-24 are spread over more than a century due to the large plateau of

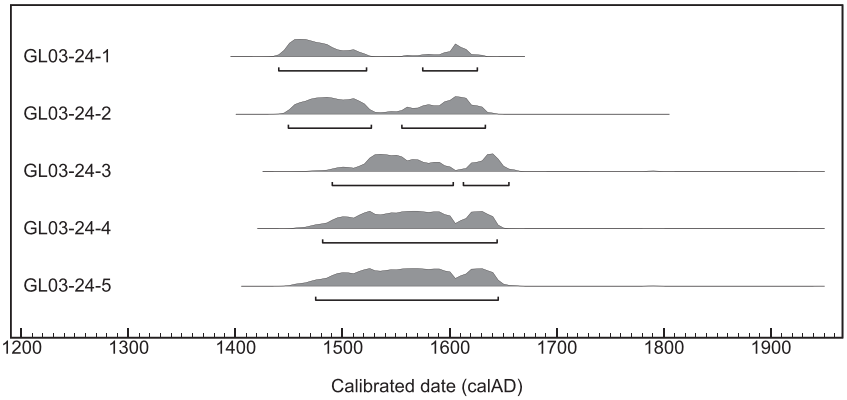

Fig. 5. Calibrated ages for the sub-samples of the cast iron GL03-24 from Glinet. Calendar age ranges were calculated using Oxcal 4.2 (Bronk Ramsey, 2009; Bronk Ramsey and Lee, 2013) and the IntCal09 calibration curve (Reimer et al., 2009).

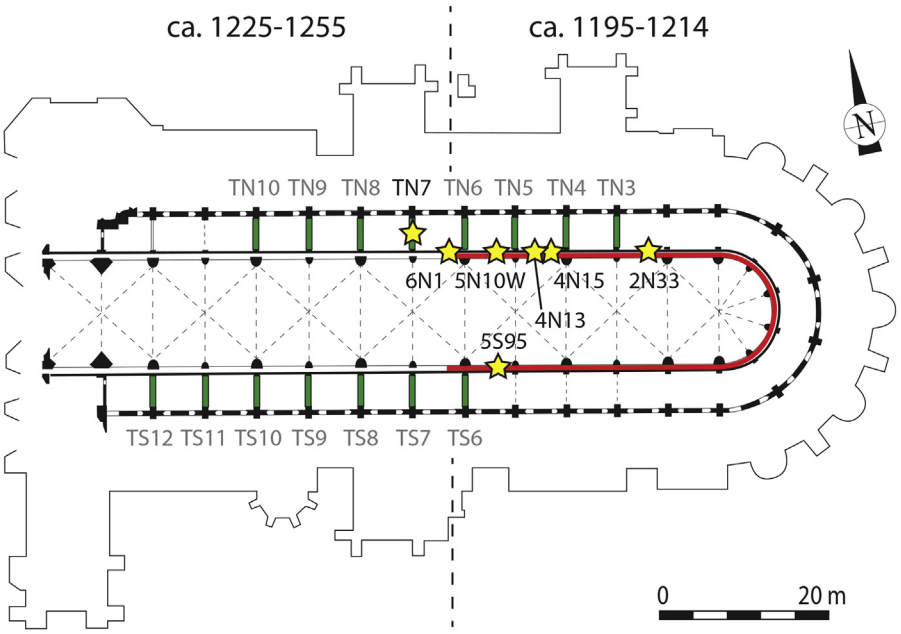

Fig. 6. Plan of Bourges Cathedral at the triforium level showing the location of the samples dated by radiocarbon (yellow stars). In red: the iron chain that encircles the choir at triforium height. In green: the tie-rods that attach the masonry of the nave pillars to the corresponding abutments in the side aisle attic. The break in the building yard is represented by the dotted line. (For interpretation of the references to colour in this figure legend, the reader is referred to the web version of this article.)

the calibration curve between 1450 and 1650 calAD (Fig. 5) but are consistent within the 2σ-range fitting into the chronological phase suggested by archaeology (*i.e.* 1480–1580 AD). Table 4 shows that the calibrated ages for the experimental bloom (RED2) are contemporaries of the last 10 years. For both cases, the reproducibility between the measurements within the iron matrix and the fact that no ageing is likely to be reported at this level suggest that no contamination is added by the geological carbon from the siderite during smelting. The reliability of the radiocarbon date of the iron is therefore ensured.

3. Set of samples from cathedral reinforcements

3.1. Bourges Cathedral

Bourges cathedral is one of the most ancient gothic monuments in which iron reinforcements were discovered. These armatures which were first identified by Branner (1989) later described by Férauge and Mignerey (1996) and more recently and precisely by L'Héritier (2012) (see Fig. 6) are present in two forms. The first is an iron chain composed of 106 links, two to three feet long, which encircles the choir at triforium height. It abruptly stops in the 6th bay of the nave (bays being counted from the east) corresponding to a well-known break in the building yard between the eastern side (*ca.* 1195–*ca.* 1214) and the western side of the building (1225–1255) (Branner, 1989). Thus, this feature is traditionally attributed to the first construction campaign. However, no contemporary historical source refers to its installation nor confirms its dating. The second set of armatures is located at the same level above the vaults of the inner aisles. It consists in 13 iron tie-rods, four to five meters long, inserted above the transverse arches spanning the vaults. They attach the masonry of the nave piers to the corresponding exterior buttresses in the earlier eastern parts as well as in the later western ones. However, archaeological observations suggest that each great pier of the nave from the second bay onward was initially reinforced by such a tie-rod. The date of their installation remains in question: whether they were part of the initial construction, whether connected to later consolidations, or linked to late medieval or modern restorations on the flying buttresses (Férauge and Mignerey, 1996)? As their precise dates are uncertain, their constructive role also remains misunderstood. We performed radiocarbon dating on seven iron samples of about 1 cm^3 taken from the chain and one piece of charcoal found in the mortar sealing the chain in the apse (Fig. 6). For the tie-rods, sampling was only possible on bar TN7, which was already fractured and, therefore, not playing any structural role in the masonry.

3.2. Beauvais Cathedral

Beauvais Cathedral is not only famous for the height of its choir (the highest in gothic architecture with 46.3 m) but also for its chaotic history. Construction began from the west in 1225. In the 1240's, it reached the triforium level and the upper parts were erected in the following decade. The choir was eventually finished in 1272 (Branner, 1962; Heyman, 1971). In November 1284 the middle vault of the choir partially collapsed and the radical reconstruction that followed lasted half a century (Murray, 1989). The extensive use of iron reinforcements in the cathedral was assessed by J.-L. Taupin (1996). These armatures include an iron chain installed over the transverse arch at the base of the hemicycle as well as a very spectacular iron structure consisting of layers of tie-rods linking the flying buttresses abutments with each otherand with the clerestory in the choir (see Fig. 7). The latter was removed by Architect J.-P. Paquet during post-WWII restorations, who mistakenly thought it was an "unnecessary and disgraceful" 19th century addition. As pointed out by Coste (1997), who questions the origins and, therefore, the role attributed to these tie-rods by the builders, it is rather unclear whether they are linked to one of the many post-1284 reparation projects or if they date back to the initial construction. According to Mark (1982), the tie-rods were installed to support the abutments – especially the intermediate pier buttresses – and prevent new accidents immediately after 1284. However, as supported by

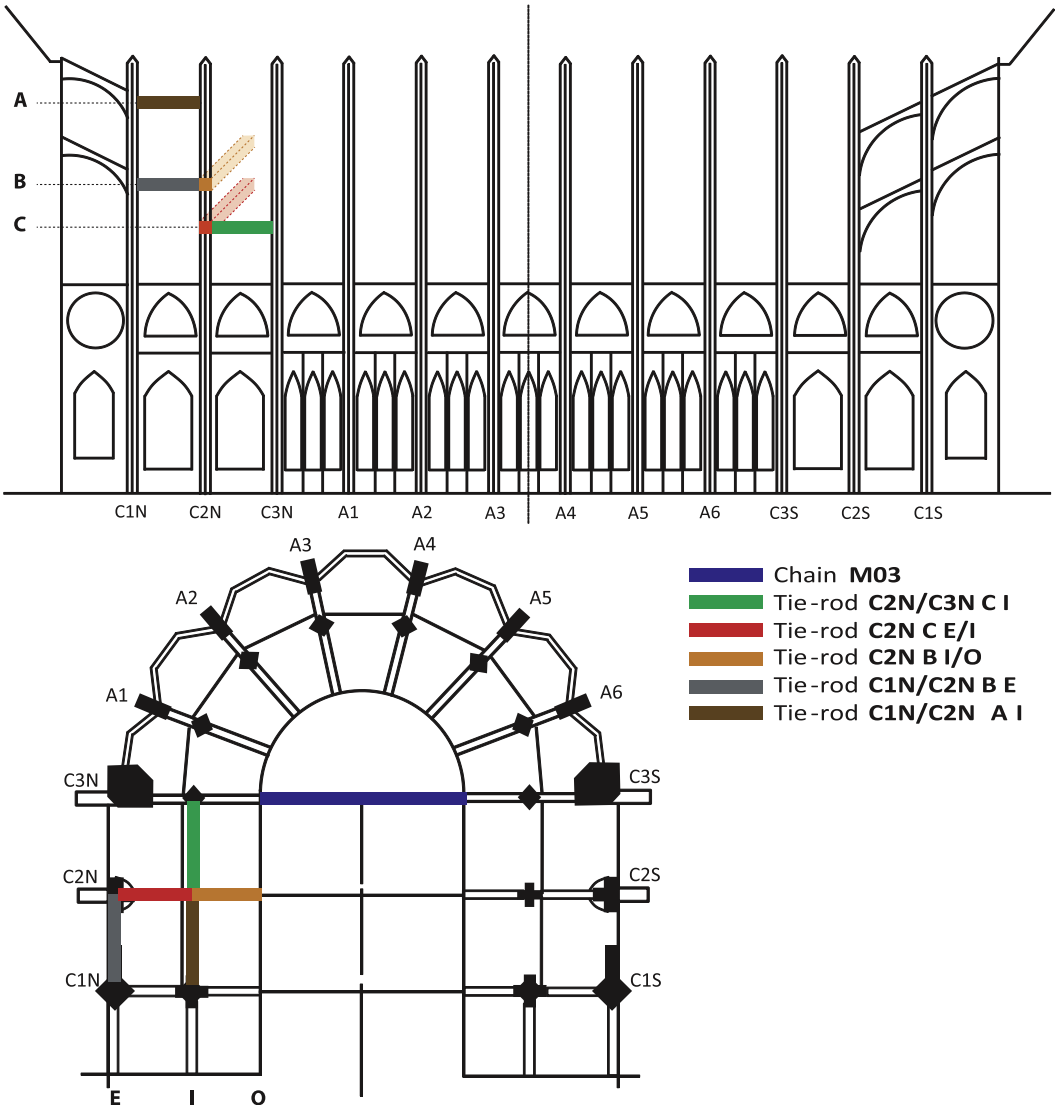

Fig. 7. Plan of the choir of Beauvais Cathedral showing the location of the tie-rods from the northern buttresses and the chain dated by radiocarbon. Up: location on the transverse cross-section of the choir. Down: location on the floor plan of the choir.

Taupin (1996), their presence as metal reinforcements since the construction in the 13th century cannot be excluded. Dating their installation has become even more complex since these tie-rods could have also been placed or replaced during an 18th century restoration campaign as some are positively dated by 18th century graffiti. Although replaced several times, the installation date of these iron ties remains undetermined and consequently the true role of iron in Beauvais Cathedral – as part of the initial

Table 5
Results of radiocarbon dating of iron armatures from Bourges Cathedral. Samples from the chain are indicated by the CH-prefix, those from the bar TN7 by the B-prefix.

Sample	Lab.ID SacA	% C	Extracted carbon content (mg)	pMC	Radiocarbon age (BP)	Calibrated age (calAD) (2σ, 95.4%)
CH-5S95	24855	0.2–0.3	1.08	88.36 ± 0.30	995 ± 25	988–1050 (70.7%) 1085–1124 (19.1%) 1136–1152 (5.6%)
CH-2N33	24856	0.2–0.3	0.92	89.38 ± 0.31	900 ± 30	1040–1110 (42.9%) 1116–1211 (52.5%)
CH-5N10W	24857	0.4–0.8	0.39	87.39 ± 0.32	1085 ± 30	894–1016
CH-6N1	24859	0–0.4	0.20	89.07 ± 0.36	930 ± 35	1022–1182
CH-4N15	24860	0.2–0.3	0.49	89.36 ± 0.34	905 ± 30	1038–1208
CH-4N13E	24861	0.2–0.3	0.52	89.90 ± 0.32	855 ± 30	1050–1082 (7.7%) 1125–1136 (1.8%) 1151–1259 (86.0%)
B-7N-1	28128	0.2	0.77	89.62 ± 0.35	880 ± 31	1041–1108 (27.6%) 1116–1222 (67.8%)
B-7N-2	28129	0.6–0.8	0.20	90.31 ± 0.38	819 ± 34	1162–1270

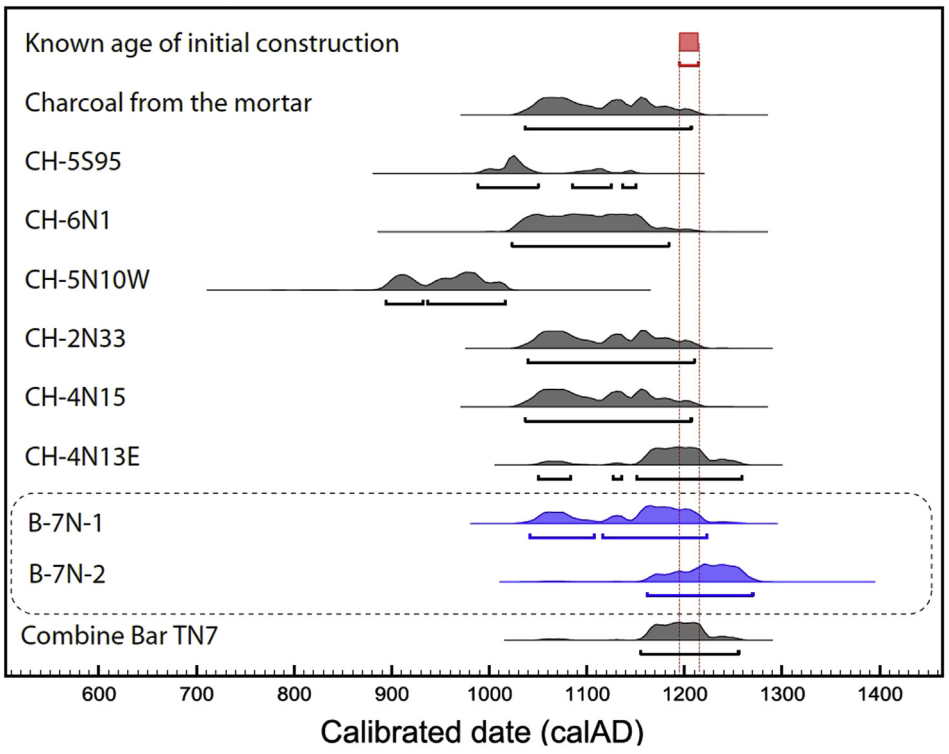

Fig. 8. Calibrated radiocarbon dates (2σ) for samples taken from the triforium chain (CH-), from the bar TN7 (B-7N-) and from the charcoal in the mortar of Bourges Cathedral. For the bar TN7, two measures were done on the same sample (in blue). They were combined with >95% probability to calculate a combined age density representative of the bar (1155–1257 calAD, 2σ). The known age of initiation of construction (1195–1214) is represented in red. Calendar age ranges were calculated using Oxcal 4.2 (Bronk Ramsey, 2009; Bronk Ramsey and Lee, 2013) and the IntCal09 calibration curve (Reimer et al., 2009). (For interpretation of the references to colour in this figure legend, the reader is referred to the web version of this article.)

constructive project or due to further consolidation in medieval or modern times – is still unknown.

Five specimens were collected from the tie-rods of the northern buttresses removed by architect J.P. Paquet and stored in the stone depot of Beauvais Cathedral. Fig. 7 shows their specific locations in the cathedral structure: peripheral tie-rods C1N/C2N B E, C1N/C2N A I and C2N/C3N C I linking the abutments of the first, second and third bays with each other at different heights and radial tie-rods C2N C E/I and C2N B I/O attaching the abutments, piers and intermediate piers of the same flying buttress. A single specimen (M03) of about 1 cm^3 was sampled from the chain above the vaults in the main attic.

4. Results for iron reinforcements and discussion

^{14}C-results for the artefacts of the Bourges Cathedral are listed in Table 5. Fig. 8 shows the calibrated temporal densities, with a 2σ range. Regarding the radiocarbon measurements, three dates overlap the chronological range of the choir construction (*ca.* 1195–*ca.* 1214) while two are older in decades (CH-5S95 & CH-6N1). However, the calibrated radiocarbon date measured for the charcoal is also slightly older (1033–1212 calAD, 2σ) and perfectly contemporary with all these iron samples. As this charcoal could not be used in the masonry before 1195, this effect could be consistent with an "old wood" effect, or due to the presence of a plateau on the calibration curve around 900 BP, which tends to spread the age density to older dates and does not allow accurate calibration. The only date significantly older is CH-5N10W. Metallographic examination of this sample revealed the presence of a welding line and further chemical investigations on the SI of this same iron sample highlighted two different chemical signatures (Fig. 9) suggesting that it was made of recycled scrap iron *i.e.* older iron, which may well age the date of the object. Apart from this recycled iron, the collected body of evidence is fully compatible with the installation of the entire chain during the construction of the choir. The obtained combined date (1155–1257 calAD, 2σ) measured for bar TN7 covers the entire construction time of the cathedral which confirms that the tie-rods were not due to later consolidation but rather linked to the initial construction phase. It

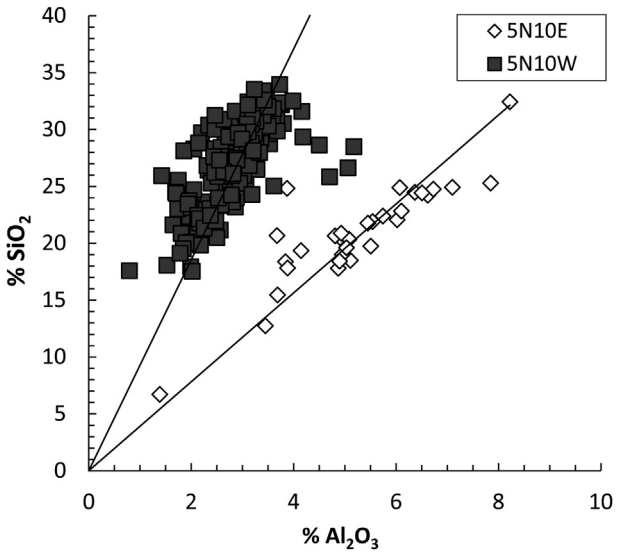

Fig. 9. Composition of the SI in both parts of the sample BOU CH5N10W indicating a recycling case.

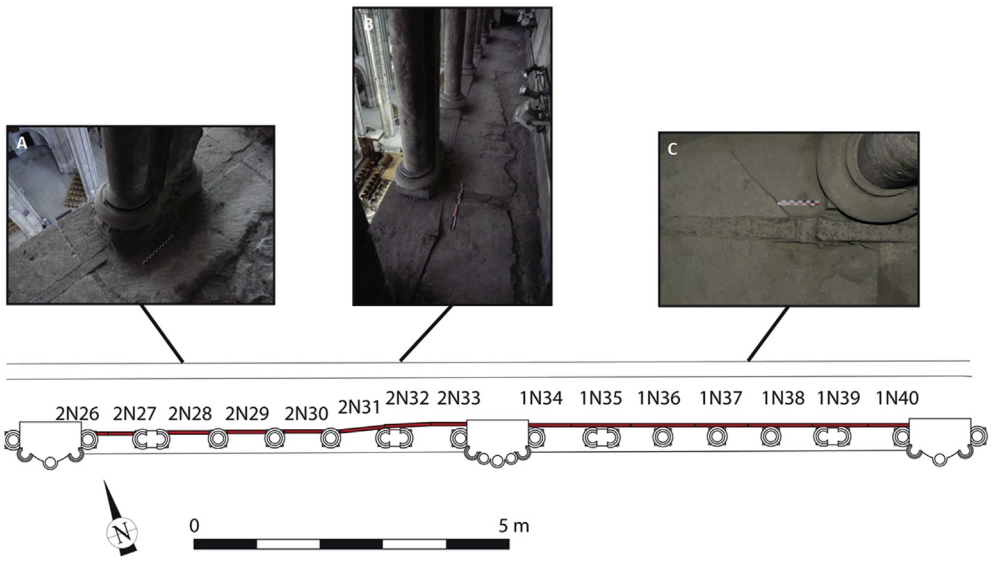

Fig. 10. Plan and photos of the iron chain (in red) between the 1st and 3rd bays showing its implantation at the column-level. Photo A: the chain runs below the triforium columns. Photo C: the chain skirts the triforium columns. (For interpretation of the references to colour in this figure legend, the reader is referred to the web version of this article.)

seems clear, and for the first time in absolute terms, that metallic elements were used since the High Gothic period as at Bourges, in the initial construction of the monuments. In fact, for this cathedral both the tie-rods in the aisles and the chain encircling the triforium date from the period of construction.

These new results have to be compared with earlier archaeological observations. As the major part of the chain runs along the triforium, below the columns, Férauge and Mignerey (1996) at first rightly claimed it should be contemporary with the cathedral's construction. However the implantation of the chain is not totally even and fine archaeological analysis reveals that it was obviously not installed during a single phase, but rather in three: the eastern parts (apse and 1st bay), southern and then northern parts (from the 2nd to the 6th bays) (L'Héritier, 2012). This is clearly observable on Fig. 10 showing a "Stratigraphic" diagram of the triforium chain assembly of Bourges cathedral between the 1st and 3rd bays showing its implantation at the level of the triforium floor. In the apse and the first bay, *i.e.* the eastern and earlier part of the choir, the chain skirts the same row of columns instead of running below them (L'Héritier, 2012). The chronological arguments of Férauge and Mignerey are therefore not valid for this part of the building. In addition, many inversions were highlighted in the succession of hooks and mortises which make up the chain assembly, especially in the northern side of the building (from the 2nd bay) (see Fig. 11) (L'Héritier, 2012). Therefore, it can be proposed that, although entirely contemporary with the initial construction phase of

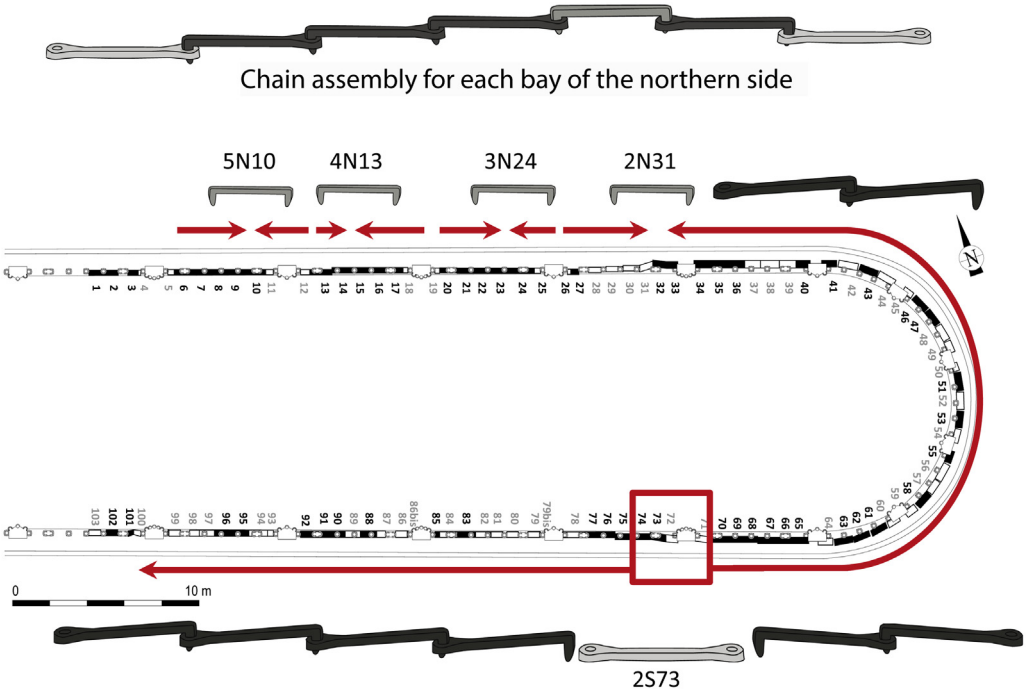

Fig. 11. "Stratigraphic" diagram of the triforium chain assembly with orientation changes.

Table 6
Results of radiocarbon dating of iron armatures from Beauvais Cathedral.

Sample	Sub-sample	Lab. ID Sac A.	% C	Extracted carbon content (mg)	pMC	Radiocarbon age (BP)	Calibrated age (calAD) (2σ, 95.4%)
M03		21123	0.3	0.17	90.56 ± 0.53	796 ± 47	1155–1288
C2N/C3N C I		21119	0.4	0.18	89.17 ± 1.23	840 ± 36	1051–1081 (5.5%) 1126–1135 (1.1%) 1152–1268 (88.8%)
C1N/C2N B E	C1N/C2N B E (1)	24853	0.3	1.40	98.51 ± 0.33	120 ± 25	Post 1680
	C1N/C2N B E (2)	24854	0.2	1.13	98.15 ± 0.34	150 ± 30	Post 1667
C2N/C1N A I		24862	0.3	0.18	98.03 ± 0.36	160 ± 30	Post 1664
C2N C E/I		19724	0.3	1.00	91.50 ± 0.25	714 ± 22	1261–1298 (94.3%) 1373–1377 (1.1%)
C2N B I/O		24851	0.2	1.23	91.59 ± 0.31	705 ± 25	1264–1301 (86.3%) 1367–1382 (9.1%)

Bourges cathedral as shown by radiocarbon dating, this chain was maybe not initially intended and was only progressively integrated into the masonry during the course of the construction, notably once the column bases were already set in the apse.

Radiocarbon results obtained on the artefacts sampled at Beauvais are presented in Table 6 and Fig. 12. Both peripheral tie-rods C1N/C2N B E and C1N/C2N A I are late modern suggesting an installation during the 18th century restoration campaign. Radial tie-rods (C2N C E/I and C2N B I/O) form a distinct overlapping group, dated from the late 13th century (1261–1298 calAD, 94.3% and 1264–1301 calAD, 86.3%) or post-mid-14th century (1373–1377 calAD, 1.1% and 1367–1382 calAD, 9.1%). The last group includes chain M03 and peripheral tie-rod C2N/C3N C I which are coherent with each other. The radiocarbon date obtained for the chain M03 (1155–1288 calAD, 2σ) is fully compatible with a recent dendrochronology study of the main roof (cutting date in 1257/1258) (Hoffsummer and Mayer, 2002), suggesting that all these armatures are indeed pre-collapse. Moreover, calendar distributions of all dated iron reinforcements seem to form three distinct chronological groups: the chain and the peripheral tie-rod C2N/C3N C I, a slightly later group of radial tie-rods, and lastly the peripheral tie-rods between the second and first bays. We tested the reliability of such a chronological sequence using OxCal4.2 by modelling radiocarbon densities according to this stratigraphic

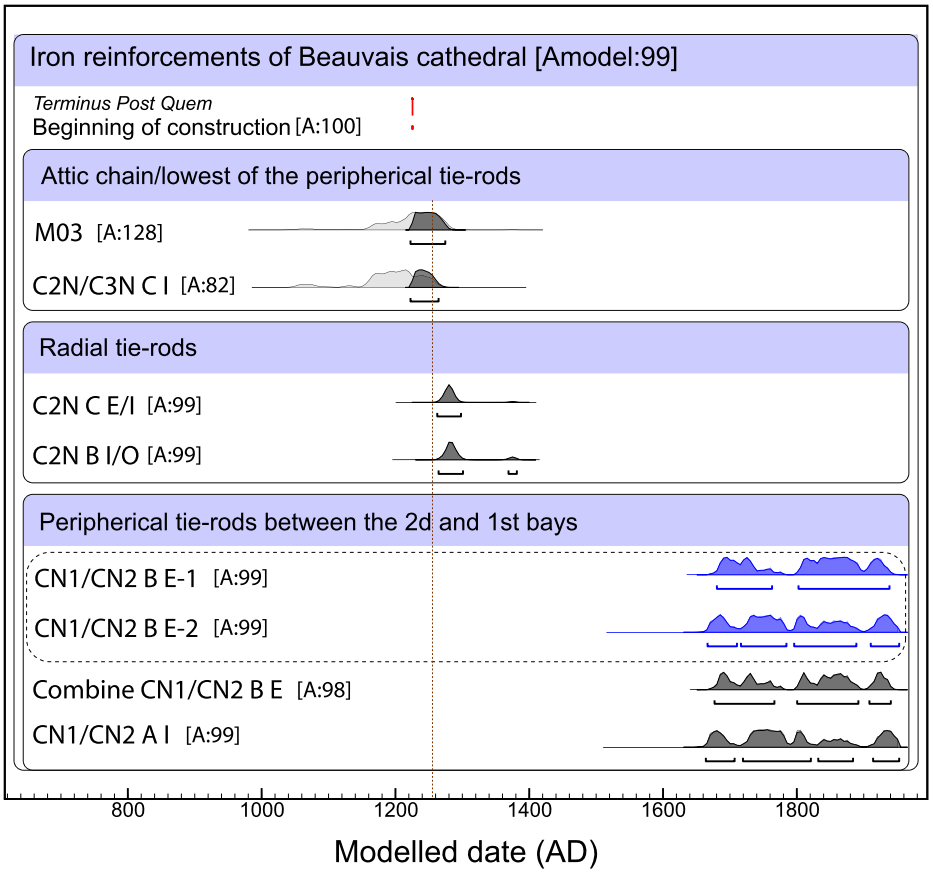

Fig. 12. Calibrated (2σ) and modelled radiocarbon dates obtained for iron samples taken from the tie-rods and the chain of Beauvais Cathedral. The dendrochronological date (1257/1258) of the main roof is indicated by the dotted brown line. For tie-rod C1N/C2N B E, two dates were obtained for the same sample (in blue). They were combined with >95% probability to calculate a combined age density representative of the bar (post 1679). The Terminus Post Quem is the known age of initiation of construction (1225). For modelled ages, a posteriori densities are shown in the darker shade; the likelihoods in the lighter shade. Calendar age ranges were calculated using Oxcal 4.2 (Bronk Ramsey, 2009; Bronk Ramsey and Lee, 2013) and the IntCal09 calibration curve (Reimer et al., 2009). (For interpretation of the references to colour in this figure legend, the reader is referred to the web version of this article.)

sequence. The very high resulting level of agreement Amodel (*ca.* 99%) shows that this chronological installation model is plausible.

According to radiocarbon dating, the chain over the transverse arch at the base of the hemicycle (M03) and the lowest of the peripheral tie-rods (C2N/C3N C I) have a high probability of being pre-1284 collapse. Therefore, the tie-rods were included in the initial design of the monument and placed between the abutments of the flying buttresses during their initial construction to regulate the space between them and prevent them from oscillating in windy conditions (Coste, 1997; Monnier, 2002). The C2N/C3N C I tie-rod is however located in the middle bay of the choir, which sustained damage in 1284 and was utterly rebuilt towards 1300 according to Murray (1989, 2011). Considering this, the most likely hypothesis is that the reconstruction of the peripheral armature system was rigorously identical to the early 13th century features and that the early 13th century tie-rods were even reused in the new construction. At least part of this peripheral reinforcement was probably restored during the 18th century (C1N/C2N BE and AI). However, it must be stressed that the latter are not at the same height as the one dating from the 13th century (see Fig. 7). They could also have been added to the lowest row of peripheral ties rods during the modern period. On the other hand, the radial tie-rods date from the late 13th century or post-mid-14th century and were seemingly placed after the 1284 collapse, either from the repair campaign, which immediately followed, or from later work in the late 14th century. However, the only well-known reparation works in the 14th century are those in the bays of the choir that concluded in 1342 (Plagnieux, 1995). No reparation or consolidation works are mentioned in textual sources between 1342 and the 16th century. Therefore, it seems reasonable that the radial tie-rods are linked to an installation towards 1300, just following the collapse. These new chronological results therefore support the hypothesis endorsed by Mark (1982) and Murray (1989, 2011), that the intermediate pier buttresses had to be reinforced to prevent another collapse and that the addition of radial elements is among the measures adopted by builders during late 13th or early 14th century reparations works (Mark, 1982) most likely to compensate for the weaknesses of the original design. In Beauvais, to succeed in one of the most daring architectural gambles of the era, the role of metal was viewed as an ally of the stone from the earliest beginnings of the building yard, and even the design phase (chain over the transverse arch at the base of the hemicycle and peripheral tie-rods). Called for since construction of the monument, and again following the first malfunction of the structure, iron was not refuted by the modern period either, as it was still employed in a significant manner in the 18th century.

5. Conclusions

A new dating methodology based on radiocarbon dating was set up to precise the role of iron reinforcements in medieval gothic monuments. This is based upon the possibility of extracting carbon from objects directly in the most carburised zones of the metal. Thus it cannot be decoupled from the metallographic and archaeometric analyses, which must be carried out systematically in studies of ferrous elements within the framework of a comprehensive approach. If this methodology is rigorously followed it appears that the radiocarbon dating of ancient ferrous alloys is reliable and paves the way for a renewal of studies in archaeology. In the case of gothic architecture this comprehensive approach to ferrous materials confirms their use from the High Gothic period. Radiocarbon analysis of iron elements from Bourges and Beauvais Cathedrals, coupled with archaeometric and archaeological data allow us to re-evaluate and refine our vision of gothic monuments building techniques through the use of iron reinforcements by medieval builders. These decisive advances in the dating of ancient ferrous materials, fully demonstrate their potential as tools for interpretation of medieval architectural monuments. More broadly, they open the way for systematic studies of other periods and regions of the world where ferrous metal played a major role. Thus, dating studies should be integrated into investigations of technical processes and the circulation of materials and products, and will in the future, contribute to the understanding of the technical, economic and social organisation of these societies.

Acknowledgements

We thank all the archaeologists who provided the objects to test our approach and, in particular, F. Téreygeol (IRAMAT), G. Pagès (ArScAn), L. Long (DRASSM), D. Arribet-Deroin (Paris-Sorbonne University) and A. Texier (LRMH). We thank C. Colliou (ARKEMINE), Cl. L'Hyver, S. Pellequer and J.-C. Méaudre (IRAMAT) for their help in performing the experimental reductions, S. Hain (LMC14) for his friendly help in the sampling for carbon extraction and finally, C. Oberlin (MOM) for the radiocarbon measurements performed in Lyon. Finally, we are grateful to Anita Quiles (IFAO) for helpful comments on the paper. This work was supported by the Ministère de la Culture et de la Communication (France) (PNRCC2010).

References

Arribet-Deroin, D., 2001. Fondre le fer en gueuses au XVIe siècle. Le haut fourneau de Glinet en pays de Bray (Normandie) (PhD thesis in Archaeology). Paris I Sorbonne, Paris.
Bernardi, P., Dillmann, P., 2005. Stone skeleton or iron skeleton: the provision and use of metal in the construction of the Papal Palace at Avignon in the 14th century. In: Bork, R. (Ed.), De Re Metallica. The Uses of Metal in the Middle Age. ASHGATE, pp. 297–315.
Beukens, R.P., Pavlish, L.A., Wilson, G.C., Farquhar, R.M., 1999. In: Young, Pollard, Budd, Ixer (Eds.), Metals in Antiquity. Archaeopress, Oxford.
Branner, R., 1962. Le Maitre de la cathédrale de Beauvais. Art Fr. 2, 77–92.
Branner, R., 1989. The Cathedral of Bourges and its Place in Gothic Architecture. MIT Press, Cambridge.
Bronk Ramsey, C., 2009. Bayesian analysis of radiocarbon dates. Radiocarbon 51 (1), 337–360.
Bronk Ramsey, C., Lee, S., 2013. Recent and planned developments of the program OxCal. Radiocarbon 55, 3–4.
Bugayev, K., Konovalov, Y., Bychkov, Y., Tretyakov, E., 2001. Iron and Steel Production. The Minerva Group, Inc.
Chapelot, O., Benoit, P., 1985. Pierre et métal dans le bâtiment au Moyen Age. EHESS, Paris.
Cheoun, M.K., Kim, J.C., Kang, J., Kim, I.C., Park, J.H., Song, Y.M., 2001. Pretreatment of iron artifacts at SNU-AMS. Radiocarbon 43 (2A), 217–219.
Cook, A.C., Wadsworth, J., Southon, J.R., 2001. AMS radiocarbon dating of ancient iron artifacts: a new carbon extraction method in use at LLNL. Radiocarbon 43 (2A), 221–227.
Cook, A.C., Southon, J.-R., Wadsworth, J., 2003a. Using radiocarbon dating to establish the age of iron-based artefacts. J. Min. Met. Mater. Soc. 55, 15–22.
Cook, A.C., Wadsworth, J., Southon, J.R., van der Merwe, N.J., 2003b. AMS radiocarbon dating of rusty iron. J. Archaeol. Sci. 30 (1), 95–101.
Coste, A., 1997. L'architecture gothique. Lectures et interprétations d'un modèle. Université de Saint Etienne, Saint Etienne.
Cottereau, E., Arnold, M., Moreau, C., Baqué, D., Bavay, D., Caffy, I., Comby, C., Dumoulin, J.-P., Hain, S., Perron, M., Salomon, J., Setti, V., 2007. Artemis, the new 14C AMS at LMC14 in Saclay, France. Radiocarbon 49 (2), 291–299.
Craddock, P.T., Wayman, M.L., Jull, A.J.T., 2002. The radiocarbon dating and authentication of iron artifacts. Radiocarbon 44 (3), 717–732.
Cresswell, R.G., 1992. Radiocarbon dating of iron artefacts. Radiocarbon 34 (3), 898–905.
Desaulty, A.M., 2008. Apport des analyses chimiques multi technique à la compréhension du comportement des éléments traces dans les filières sidérurgiques anciennes. Application des études de provenance et à la distinction des procédés. Le cas du Pays de Bray normand (PhD Thesis of the Université Technologique de Belfort-Montbéliard).
Dillmann, P., 2009. De Soissons à Beauvais : le fer des cathédrales de Picardie, une approche archéométrique. In: Timbert, A. (Ed.), L'Homme et la Matière : l'emploi du plomb et du fer dans l'architecture gothique, pp. 93–112. Picard, Paris.
Dillmann, P., L'Héritier, M., 2007. Slag inclusion analyses for studying ferrous alloys employed in French medieval buildings: supply of materials and diffusion of smelting processes. J. Archaeol. Sci. 34 (11), 1810–1823.

Disser, A., Dillmann, Ph, Bourgain, C., L'Héritier, M., Vega, E., Bauvais, S., Leroy, M., 2014. Iron reinforcements in Beauvais and Metz Cathedrals: from bloomery or finery ? The use of logistic regression for differentiating smelting processes. J. Archaeol. Sci. 42, 315–333.
Erlande-Brandenburg, A., 1996. L'architecture rayonnante et le métal. Doss. d'archéol. 219, 46–53.
Férauge, M., Mignerey, P., 1996. L'utilisation du fer dans l'architecture gothique : l'exemple de la cathédrale de Bourges. Bull. Monum. T154 (II), 129–146.
Fluzin, P., Bauvais, S., Berranger, M., Pagès, G., Dillmann, P., 2011. The multidisciplinary approach (archaeology and archaeometry) to bloomsmithing activities in France: examples of results from the last twenty years. In: Hosek, J., Cleere, H., Mihok, L. (Eds.), The Archaeometallurgy of Iron – Recent Developments in Archaeological and Scientific Research. The Institute of Archaeology of the ASCR, Prague, pp. 223–236.
Forbes R.J., 1955, 1963, 1964., In: Brill, E.J., (Ed.), Studies in Ancient Technology, Leiden, 199, 215, 253, 288, 295
Hatté, C., Poupeau, J.-J., Tannau, J.-F., Paterne, M., 2003. Development of an automated system for preparation of organic samples. Radiocarbon 45 (3), 421–430.
Heyman, J., 1971. Beauvais cathedral? Trans. Newcom. Soc. XL, 15–36.
Hoffsummer, P., Mayer, J., 2002. Les charpentes du XIe au XIXe siècle, Typologie et évolution en France du Nord et en Belgique. Monum-ed. du Patrimoine, Paris.
Hüls, C.M., Grootes, P.M., Nadeau, M.-J., Bruhn, F., Hasselberg, P., Erlenkeuser, H., 2004. AMS radiocarbon dating of iron artefacts. Nucl. Instrum. Methods Phys. Res. Sect. B 223–224, 709–715.
Kusimba, C.M., Killick, D.J., Cresswell, R.G., 1994. Indigenous and imported metals at Swahili sites on the Coast of Kenya. In: Childs, S.T. (Ed.), Society, Culture and Technology in Africa. MASCA, University of Pennsylvania Museum of Archaeology and Anthropology, Philadelphia, pp. 63–79.
L'Héritier, M., 2007. L'utilisation du fer dans l'architecture gothique. Les cas de Troyes et de Rouen (PhD thesis of Archéologie). Sorbonne, Paris.
L'Héritier, M., 2012. Les armatures de fer de la cathédrale de Bourges à l'épreuve de l'archéologie et de l'archéométrie Octobre 2012, Bourges.
L'Héritier, M., Dillmann, P., Benoit, P., 2010. The use of ferrous alloys for the building of gothic churches. Role, origins and production of the metal, through the examples of Rouen and Troyes. Hist. Metall. 44 (1), 21–35.
Leroy, S., Cohen, S.X., Verna, C., Gratuze, B., Téreygeol, F., Fluzin, P., Bertrand, L., Dillmann, P., 2012. The medieval iron market in Ariège (France). Multidisciplinary analytical approach and multivariate analyses. J. Archaeol. Sci. 39 (4), 1080–1093.
Mark, R., 1982. Experiments in Gothic Structure. MIT press, Cambridge.
Monnier, E., 2002. Des monuments qui jouent avec la mécanique. In: Les cahiers de Science et Vie, vol. 69. Sciences et techniques des bâtisseurs de cathédrales, pp. 12–21.
Murray, S., 1989. Beauvais Cathedral: Architecture of Transcendence. Princeton University Press, Princeton.
Murray, S., 2011. Back to Beauvais (2009). In: Bork, R., Clark, W.W., McGehee, A. (Eds.), New Approaches to Medieval Architecture, Medieval Technology, Science and Art. Ashgate, pp. 45–60.
Nakamura, T., Hirasawa, M., Igaki, K., 1995. AMS radiocarbon dating of ancient oriental iron artefacts at Nagoya University. Radiocarbon 37 (2), 629–636.
Oinonen, M., Haggren, G., Kaskela, A., Lavento, M., Palonen, V., Tikkanen, P., 2009. Radiocarbon dating of iron: a northern contribution. Radiocarbon 51 (2), 873–881.
Pagès, G., Dillmann, P., Fluzin, P., Long, L., 2011. A study of the Roman iron bars of Saintes-Maries-de-la-Mer (Bouches-du-Rhône, France). A proposal for a comprehensive metallographic approach. J. Archaeol. Sci. 38, 1234–1252.
Plagnieux, P., 1995. La date et les architectes de la restauration de la cathédrale de Beauvais après l'effondrement de 1284. Bull. Soc. natl. Antiq. Fr. 403–409.
Reimer, P.J., Baillie, M.G.L., Bard, E., Bayliss, A., Beck, J.W., Blackwell, P.G., Bronk Ramsey, C., Buck, C.E., Burr, G.S., Edwards, R.L., Friedrich, M., Grootes, P.M., Guilderson, T.P., Hajdas, I., Heaton, T.J., Hogg, A.G., Hughen, K.A., Kaiser, K.F., Kromer, B., McCormac, F.G., Manning, S.W., Reimer, R.W., Richards, D.A., Southon, J.R., Talamo, S., Turney, C.S.M., van der Plicht, J., Weyhenmeyer, C.E., 2009. IntCal09 and Marine09 radiocarbon age calibration curves, 0–50,000 years cal BP. Radiocarbon 51 (4), 1111–1150.
Scharf, A., Kretschmer, W., Morgenroth, G., Uhl, T., Kritzler, K., Hunger, K., Pernicka, E., 2004. Radiocarbon dating of iron artefacts at the Erlangen AMS facility. Radiocarbon 46 (1), 175–180.
Scharf, A., Kretschmer, W., Uhl, T., Kritzler, K., Hunger, K., Pernicka, E., 2005. Radiocarbon dating of iron artefacts at the Erlangen AMS-facility. Nucl. Instrum. Methods Phys. Res. Sect. B 240 (1–2), 478–482.
Stuiver, M., Polach, H., 1977. Discussion: reporting of 14C data. Radiocarbon 19 (3), 355–363.
Taupin, J.-L., 1996. Le fer dans les cathédrales. Monumental 13, 18–27.
Téreygeol, F., 2011. Le Castel-Minier (Aulus-les-Bains), Document Final de Synthèse, tapuscrit, SRA Midi-Pyrénées.
Timbert, A., 2009. L'homme et la matière: l'emploi du plomb et du fer dans l'architecture gothique. Picard, Paris.
Van der Merwe, N.J., Stuiver, M., 1968. Dating iron by the Carbon-14 method. Curr. Anthropol. 9 (1), 48–53.